

1 Intra-oropharyngeal food transport and
2 swallowing in white-spotted bamboo
3 sharks

4

5 Noraly M.M.E. van Meer^{1*}, Hannah I. Weller², Armita R. Manafzadeh², Elska B.
6 Kaczmarek², Bradley Scott³, Sander W.S. Gussekloo¹, Cheryl D. Wilga⁴, Elizabeth L.
7 Brainerd² and Ariel L. Camp^{2,5}

8

9 ¹Experimental Zoology Group, Wageningen University, Wageningen, The Netherlands

10 ²Department of Ecology and Evolutionary Biology, Brown University, Providence, RI, USA

11 ³Department of Animal Biology, University of Illinois, Urbana-Champaign, IL, USA

12 ⁴Department of Biological Sciences, University of Alaska Anchorage, Anchorage, AK, USA

13 ⁵Institute of Ageing and Chronic Disease, University of Liverpool, Liverpool, United Kingdom

14

15 *Author for correspondence (e-mail: noralymmevanmeer@gmail.com)

16 Abstract

17 Despite the importance of intraoral food transport and swallowing, relatively few
18 studies have examined the biomechanics of these behaviors in non-tetrapods, which lack a
19 muscular tongue. Studies show that elasmobranch and teleost fishes generate water
20 currents as a 'hydrodynamic tongue' that presumably transports food towards and into the
21 esophagus. However, it remains largely unknown how specific musculoskeletal motions
22 during transport correspond to food motion. Previous studies of white-spotted bamboo
23 sharks (*Chiloscyllium plagiosum*) hypothesized that motions of the hyoid, branchial arches,
24 and pectoral girdle, generate caudal motion of the food through the long oropharynx of
25 modern sharks. To test these hypotheses, we measured food and cartilage motion with
26 XROMM during intra-oropharyngeal transport and swallowing (n=3 individuals, 2-3 trials per
27 individual). After entering the mouth, food does not move smoothly toward the esophagus,
28 but rather moves in distinct steps with relatively little retrograde motion. Caudal food motion
29 coincides with hyoid elevation and a closed mouth, supporting earlier studies showing that
30 hyoid motion contributes to intra-oropharyngeal food transport by creating caudally-directed
31 water currents. Little correspondence between pectoral girdle and food motion was found,
32 indicating minimal contribution of pectoral girdle motion. Transport speed was fast as food
33 entered the mouth, slower and step-wise through the pharyngeal region and then fast again
34 as it entered the esophagus. The food's static periods in the step-wise motion and its high
35 velocity during swallowing could not be explained by hyoid or girdle motion, suggesting these
36 sharks may also use the branchial arches for intra-oropharyngeal transport and swallowing.

37 Introduction

38 After capturing food, there are at least two equally important steps in feeding: transport and
39 swallowing. Intra-oropharyngeal transport is the process of moving food after initial prey
40 capture, from the oral cavity, through the pharyngeal cavity and towards the esophagus.
41 Food is then swallowed when it enters the esophagus. Both transport and swallowing require
42 a force to move the food caudally. In mammals, for example, this force is provided by the
43 tongue, which transports both liquids and solids towards the esophagus like, in the words of
44 Hiimae and Crompton (1985), a “conveyor belt”. The food bolus is swallowed by
45 stereotypical activation and de-activation of muscles of the hyoid, tongue, soft palate and
46 pharyngeal constrictors (Hiimae and Crompton, 1985). Similar behavior has also been
47 observed in some lissamphibians (Bemis, 1986; Reilly and Lauder, 1990), and sauropsids,
48 unless the tongue has been adapted as a chemosensory organ, as in snakes (Kley and
49 Brainerd, 2002). In some cases, a ‘throw-and-catch’ mechanism may be used, which
50 involves throwing the food upward and opening the oropharyngeal cavity wide, so the food
51 falls into the esophagus (Herrel et al., 1996; Herrel et al., 1997; Schaerlaeken et al., 2011).
52 The throw-and-catch mechanism is considered the most basal feeding pattern of birds
53 (Zweers et al., 1994) and occurs in birds that possess relatively small tongues with no
54 remarkable features, such as the greater rhea (Gusseklou and Bout, 2005).

55 In contrast, fish do not possess a mobile, muscular tongue, and they generally do not
56 feed in air. Feeding in water poses a quite different set of challenges and opportunities
57 compared to feeding on land (Heiss et al., 2018). Instead of using a muscular tongue, fish
58 can use the water to their advantage by creating a ‘hydrodynamic tongue’ (Liem, 1990). This
59 tongue is not an anatomical structure, but rather water currents are generated inside the
60 mouth to reposition and transport food. The water flows are generated by expansion or
61 contraction of the oropharyngeal cavity, for example by elevation or depression of the hyoid
62 (Dean et al., 2005; Michel et al., 2015). This hydrodynamic tongue behavior has been
63 observed in a broad spectrum of species within the actinopterygians and lungfish (Bemis,
64 1986; Gillis and Lauder, 1995; Lauder, 1983; Michel et al., 2015). In addition, a
65 hydrodynamic tongue has been observed in aquatic amphibians, turtles, and some marine
66 mammals, even though they also possess a muscular tongue (Gillis and Lauder, 1994;
67 Levine et al., 2004; Natchev et al., 2009; Werth, 2000). In addition to the hydrodynamic
68 tongue, ray-finned fishes can use their pharyngeal jaws to grasp, transport and process food
69 (Lauder, 1983; Mehta and Wainwright, 2007; Vandewalle et al., 2000; Wainwright, 2005).

70 Sharks, like ray-finned fishes, do not possess a muscular tongue, and they do not
71 possess pharyngeal jaws either. Sharks also have an exceptionally long oropharyngeal
72 cavity, spanning the space from the jaws through the hyoid region and across the five

73 branchial arches, which are caudal to the cranium, to the even more caudally-located
74 pectoral girdle (Fig. 1). In contrast, in actinopterygians the branchial arches and pectoral
75 girdle are ventral to the cranium forming a relatively short compact oropharyngeal cavity.
76 Hence, sharks face a bigger challenge as they need to transport food a relatively longer
77 distance than actinopterygian fishes.

78 Studies on fluid pressure and fluid dynamics of feeding behavior in white-spotted
79 bamboo sharks (*Chiloscyllium plagiosum*) found they use suction to capture prey and to
80 transport it from the jaws into the oropharyngeal cavity (Nauwelaerts et al., 2008; Wilga and
81 Sanford, 2008), essentially using suction feeding and a hydrodynamic tongue like ray-finned
82 fishes. Suction is generated by coordinated expansion of the oropharyngeal cavities
83 (Ramsay and Wilga, 2017; Scott et al., 2019; Wilga, 2008; Wilga, 2010; Wilga and Sanford,
84 2008; Wilga et al., 2012), which results in fluid flows that move the food from the surrounding
85 environment or jaws into the pharynx (Nauwelaerts et al., 2007; Nauwelaerts et al., 2008;
86 Wilga and Motta, 1998a; Wilga and Motta, 1998b; Wilga and Motta, 2000; Wilga and
87 Sanford, 2008; Wilga et al., 2007; Wilga et al., 2012). These previous studies have inferred
88 food position within the long oropharynx, but food position has not been measured explicitly
89 during intra-oropharyngeal transport and swallowing.

90 Despite this evidence of sharks using a hydrodynamic tongue driven by hyoid
91 motions to transport food initially from the jaws into the oropharynx, it remains unclear how
92 musculoskeletal and fluid motions contribute to specific food motion within the oropharynx.
93 Prior studies have shown that expansion and compression of the hyoid and branchial arches
94 by their associated musculature during food processing and transport are responsible for the
95 positive and negative pressure changes and unsteady flows in the intra-oropharyngeal cavity
96 (Wilga, 2010; Wilga and Motta, 1998a; Wilga and Motta, 1998b; Wilga and Sanford, 2008;
97 Wilga et al., 2012). Expansion of the hyoid arch is hypothesized to generate fluid flows,
98 which transport the food down the center of the oropharyngeal cavity from the jaws to the
99 esophagus (Wilga and Sanford, 2008; Wilga et al., 2012). However, the location of the food
100 has not been measured during these behaviors, so the proposed relationship between hyoid
101 and food motion has not been tested. The pharynx is hypothesized to function as a sink, with
102 the branchial arches expanding to receive the incoming bolus of water and food (Wilga and
103 Sanford, 2008; Wilga et al., 2012). A more recent study showed that the pectoral girdle is
104 mobile and contributes to suction feeding in bamboo sharks (Camp et al., 2017). Camp et al.
105 also hypothesized that the location of the pectoral girdle at the back of the elongated pharynx
106 (Fig. 1) might allow caudoventral pectoral girdle motion (retraction) to contribute to
107 pharyngeal cavity expansion and flow generation for food transport. However, the actual food
108 motions relative to hyoid, branchial and pectoral girdle motions during food transport remain
109 hypothetical as the head is covered with thick skin and muscle making direct, precise

110 measurements difficult without X-ray imaging (but see use of sonomicrometry for suction
111 feeding, (Wilga and Sanford, 2008)).

112 Here, we use X-ray Reconstruction of Moving Morphology (XROMM) to test whether
113 motions of the hyoid, pectoral girdle, or both contribute substantially to intra-oropharyngeal
114 transport and swallowing in white-spotted bamboo sharks. XROMM is a technique that
115 combines biplanar X-ray video and CT-scans to reconstruct *in vivo* 3D skeletal kinematics
116 (Brainerd et al., 2010). We use an existing XROMM dataset collected for studying suction
117 feeding (Camp et al., 2017; Scott et al., 2019) that also incidentally collected some complete
118 sequences of transport and swallowing. Branchial arch cartilages were not marked so the
119 hypothesized contributions of those elements cannot be tested directly, but consistent food
120 transport in the absence of hyoid or pectoral girdle motions would lend support to
121 contributions from motions of the branchial arches. As noted above, food transport and
122 swallowing are equally important for nutrition and survival as food capture, and this study will
123 test existing hypotheses for the roles of the hyoid arch and pectoral girdle in transport and
124 swallowing in a member of a functionally and phylogenetically important vertebrate group.
125 We hypothesize that hyoid expansion will create an unsteady flow that moves the food down
126 the center of the oropharyngeal cavity from the jaws to the esophagus. We also hypothesize
127 that pectoral girdle depression will assist in the creation of the flow that moves the food
128 towards the esophagus. Sharks are functionally important because they lack the pharyngeal
129 jaws that are thought to assist transport and swallowing in many ray-finned fishes and they
130 are phylogenetically important as the outgroup to Osteichthyes, including lobe-finned fishes
131 and tetrapods. These data will add to an emerging evolutionary synthesis of food transport
132 and swallowing mechanisms in Gnathostomata that has thus far not included Chondrichthyes
133 (Heiss et al., 2018).

134

135 Methods

136 Animals

137 Cartilage and food kinematics were quantified using XROMM for three white-spotted bamboo
138 sharks, *Chiloscyllium plagiosum* (Bennett 1830). Total body lengths were 78.6, 79.2 and 85.0
139 cm for Bam02, Bam03 and Bam04, respectively. These same individuals were used in prior
140 XROMM studies of suction feeding (Camp et al., 2017; Scott et al., 2019) and trials for all
141 three studies were collected simultaneously. Therefore, all methods follow those two prior
142 studies and are described here only briefly. All animal care and experiments were approved
143 by the Institutional Animal Care and Use Committees of Brown University and the University
144 of Rhode Island. Each shark was anaesthetized (Wilga and Sanford, 2008) and tungsten
145 carbide conical markers (Kambic et al., 2014) were implanted in the chondrocranium,

146 pectoral girdle (for Bam04 only), and left palatoquadrate (upper jaw), Meckel's cartilage
147 (lower jaw), hyomandibula and ceratohyal (Camp and Brainerd, 2014). All sharks recovered
148 fully and resumed normal feeding behaviors prior to data collection. We follow the anatomical
149 terminology of Wilga and Sanford (Wilga and Sanford, 2008), but we will use the term 'oral
150 cavity' to refer to the buccal and hyoid cavities together.

151

152 Data collection

153 The sharks were fed small (less than half of gape width) pieces of squid or herring marked
154 with a single tantalum or ceramic bead in the center of the prey item while being filmed within
155 the oblique, biplanar field of view of two X-ray machines (Imaging Systems and Service,
156 Painesville, OH, USA), which generated X-rays at 110–120 kV and 100 mA. The resulting X-
157 ray videos were recorded at 320 or 330 frames per second by Phantom v.10 high-speed
158 cameras (Vision Research, Wayne, NJ, USA). Video and calibration data are stored with
159 their essential metadata on the XMAPortal (<http://xmaportal.org>) in accordance with
160 best practices for video data management in organismal biology (Brainerd et al., 2017).

161 As noted above, we used an existing XROMM dataset collected for studying suction
162 feeding (Camp et al., 2017; Scott et al., 2019) that also incidentally collected some complete
163 sequences of transport and swallowing. Hence, the sample size for this study is not large;
164 there were only 7 trials across 3 individuals (n=2 for Bam02 and Bam03, n = 3 for Bam04) in
165 which the food was marked and the entire feeding bout—from capture to swallowing—was
166 visible. However, given the substantial difficulty of marking animals and collecting XROMM
167 data, it is worthwhile to make use of these data to gain insights that are unobtainable in any
168 other way at this time.

169 After the first day of trials, the sharks were anesthetized and *in vivo* computed
170 tomography (CT) scans (FIDEX CT, Animage, Pleasanton, CA, USA) were taken of all
171 sharks (resolution = 416 x 416 or 448 x 448 pixels; slice thickness = 0.185 mm), and mesh
172 models of the cartilages and markers were created in OsiriX (Pixmeo, Geneva, Switzerland)
173 or Horos (horosproject.org) and Geomagic Studio (11, Geomagic, Inc., Triangle Park, NC,
174 USA).

175 The biplanar X-ray videos were undistorted, calibrated, and all markers in the
176 cartilages and food were tracked in XMALab (Knörlein et al., 2016) with a precision of 0.15
177 mm. This precision of marker tracking was calculated by taking the mean of the standard
178 deviations of marker-to-marker distance pairs for markers within each rigid body of every
179 trial, and subsequently calculating the mean across all trials (Brainerd et al., 2010; Knörlein
180 et al., 2016). Using the XYZ coordinates of the cartilage markers from the X-ray videos, and
181 the anatomical location of each marker from the CT scan, rigid body transformations were

182 calculated and filtered (low-pass Butterworth, 50 Hz cut-off frequency) for each cartilage. In
183 addition, XYZ coordinates of the food marker were exported from XMALab.

184

185 Data visualization and analysis

186 For each feeding trial, the mesh models of the cartilages were animated with the rigid body
187 transformations in Maya (2016, Autodesk, San Rafael, CA, USA) to create an XROMM
188 animation. The unmarked pectoral girdles in Bam02 and Bam03 were animated by Scientific
189 Rotoscoping (Gatesy et al., 2010). The pectoral girdle was clearly visible in the X-ray images
190 (Camp et al., 2017) and a mesh model of the pectoral girdle was aligned with the image of its
191 position in the two X-ray videos. The result was a single skeletal animation combining
192 marker-based (Brainerd et al, 2010) and markerless (Gatesy et al., 2010) XROMM for each
193 feeding trial.

194 Within each animated feeding trial, virtual landmarks were selected (by parent
195 constraining a locator to the mesh cartilage model) at the rostroventral tips of the upper jaw,
196 lower jaw, ceratohyal and the ventral tip of the pectoral girdle. An anatomical coordinate
197 system (ACS) was placed in the middle of the chondrocranium with the X-axis aligned
198 rostrocaudally, the Y-axis aligned medio-laterally (left-right) and the Z-axis aligned
199 ventrodorsally. This ACS served as a frame of reference for measuring food translation and
200 cartilage landmark displacements relative to the cranium.

201

202 Kinematic measurements

203 The XYZ coordinates of the food were re-calculated relative to the chondrocranial ACS.
204 Translations in the rostrocaudal axis were normalized by the distance between the jaw tips
205 and the pectoral girdle to correct for size differences among individuals. This distance
206 represents the length of the entire oropharyngeal cavity, and therefore allowed us to express
207 food motion relative to how much of the cavity it had travelled. The oropharyngeal cavity
208 length (mouth-pectoral girdle distance) was calculated for each trial as the difference
209 between the rostral position of the food when it entered the mouth and the position of the
210 food when it passed the pectoral girdle and then averaged for each shark. Dissection of
211 Bam04 confirmed that the opening to the esophagus lies within the plane of the pectoral
212 girdle, i.e. medial to both scapulae and slightly dorsal to the coracoid (Fig. S1), so we used
213 the position of the pectoral girdle as a proxy for the location of the entrance to the
214 esophagus. Thus, a normalized rostrocaudal translation value of 0 indicates the food is at the
215 rostral tip of the jaws and about to be captured, and a value of 1 indicates that the food is
216 passing the pectoral girdle, entering the esophagus and being swallowed. Non-normalized

217 rostrocaudal translations of the food were used to calculate the velocity of the food motion
218 toward the esophagus.

219 Cartilage motions were described by the displacement of virtual landmarks, relative to
220 the chondrocranial ACS. Rostrocaudal cartilage displacements were normalized for mouth-
221 pectoral girdle distance, as described above for the food. The normalized displacements
222 allowed us to more directly compare motions of the cartilages to those of the food. Gape was
223 calculated as the distance between the upper and lower jaw landmarks. We confirmed that
224 rotation of the pectoral girdle relative to the body plane (as measured previously in Camp et
225 al., 2017) and the dorsoventral displacement of the coracoid bar (relative to the
226 chondrocranium ACS) showed the same pattern.

227

228 Results

229 Across the seven trials in this study, all sharks used suction feeding to draw food directly into
230 the oral cavity; none of the sharks captured the food between the teeth or manipulated food
231 with the jaws, likely because the food pieces were deliberately cut to no more than half-gape
232 width for the suction-feeding studies (Camp et al., 2017; Scott et al., 2019). We observed no
233 difference in transport and swallowing between herring and squid pieces.

234 After the food entered the mouth ($x = 0$ in Fig. 2), it initially moved caudally through
235 the oral cavity in a smooth trajectory, with very little lateral or dorsoventral motion in the first
236 30% of oropharyngeal length (the length from the jaw tip to the pectoral girdle) ($x \leq 0.3$ in Fig.
237 2); approximately at the level of the hyomandibula-cranial articulation (Figs. 1-2). Then the
238 food continued to move caudally as well as laterally in most trials (Fig. 2B) and ventrally in
239 some trials (Fig. 2A). However, motions in both the lateral and the dorsoventral axes were
240 relatively small during this period. After the food reached 80% of oropharyngeal length ($x \geq$
241 0.8 in Fig. 2), it moved back toward the mid-sagittal plane, and in all trials there was a small
242 rostral translation just before or after the food was swallowed ($x = 1$ in Fig. 2). For an
243 example of a trial, see Movie 1 and 2.

244 When we isolated the rostrocaudal translations of the food, we observed a step-wise
245 movement (Fig. 3). The food moved rapidly in a caudal direction during the initial suction
246 capture event, and then continued to move in a series of smaller, discontinuous motions
247 where it moved caudally, then stopped or moved slightly rostrally, and then moved caudally
248 again until the food reached the esophagus. During the relatively stationary phases, the food
249 moved slightly anteriorly in most cycles. In one case (Bam03, Trial 02), the food moved
250 nearly equally in the rostral and caudal directions through several cycles, making no
251 progress toward the esophagus until about 80% of the duration of the feeding bout, at which

252 time it began the step-wise motion seen in the other trials and progressed into the
253 esophagus (Fig. 3).

254 During feeding, rostrocaudal translation of the food was accompanied by dorsoventral
255 motion of the ceratohyal and the coracoid bar and changes in gape (Fig. 4), as measured by
256 virtual landmark displacements. During prey capture, all sharks depressed (i.e., ventrally
257 displaced relative to the chondrocranium) the ceratohyal as the gape closed and the food
258 accelerated into the oral cavity. One shark, Bam02, slightly elevated the coracoid bar and
259 then depressed it, and the gape closed after the food moved caudally.

260 After capture, the step-wise food motions began as all sharks closed the gape and
261 elevated (i.e., dorsally displaced relative to the chondrocranium) the ceratohyal while the
262 food was transported caudally. The coracoid bar was either depressed or elevated with the
263 ceratohyal; the direction of motion varied between individuals. In general, Bam03 and Bam04
264 elevated, while Bam02 depressed the coracoid bar. The ceratohyal also elevated during
265 swallowing as the mouth was closed, but ceratohyal and coracoid bar translations were
266 generally smaller than during food transport.

267 In Trial 02 from Bam02, the shark depressed the ceratohyal and coracoid bar during
268 intra-oropharyngeal transport while the gape was open, as it did during capture (Fig. S2).
269 When the shark combined a closed gape and hyoid elevation, the step-wise food transport
270 was successful, and the food was swallowed.

271 In all trials, the food particle made an additional rostrally directed, high-velocity
272 movement when it was near or inside the esophagus, before it continued caudally down the
273 esophagus towards the stomach (Fig. 4, 5). As the position of the esophageal sphincter was
274 not marked in the X-ray video, it is unclear whether this movement occurred just before or
275 after the food entered the esophagus.

276 The velocities of the food trajectories through the oropharynx show four phases of
277 food motion (Fig. 5). The first phase, prey capture, was the fastest, with peak velocities of 55-
278 270 cm s⁻¹ (mean of 145 cm s⁻¹), as the food moved through about the first half of the
279 oropharynx (up to $x = 0.5$). Food velocity then dropped to a mean of 5.4 cm s⁻¹ (range of 0.2-
280 71 cm s⁻¹) between $x = 0.5$ and 0.8 during intra-oropharyngeal transport in Phase 2, after
281 which it increased again during swallowing in Phase 3, reaching local peaks of 29-130 cm s⁻¹
282 (mean of 74 cm s⁻¹) near the opening to the esophagus ($x = 1.0$). Peak velocities in Phase 3
283 were in between those of Phase 2 and Phase 1. In Phase 4, when the food has been
284 swallowed, it slowed down inside the esophagus to a velocity comparable to those seen in
285 the middle of the pharynx in Phase 2.

286

287 Discussion

288 Until now it was unclear how food motion corresponds to the musculoskeletal motions that
289 sharks use to transport food through the long oropharynx, without either a muscular tongue
290 or pharyngeal jaws. We show that white-spotted bamboo sharks transport food items in a
291 series of distinct steps, where the food alternates between phases of caudal motion and
292 relative immobility (Fig. 3). This step-wise food transport has not previously been observed in
293 sharks, as the muscles and skin surrounding the oropharynx make it difficult to directly and
294 precisely measure food location without X-ray imaging. Our results support the hypothesis
295 that motions of the hyoid—and not the pectoral girdle—generate caudally-directed unsteady
296 water currents to move food towards the esophagus. The branchial arches may be
297 responsible for the food’s relatively static periods during step-wise transport and contributing
298 to its relatively high velocity during swallowing, as neither hyoid nor pectoral girdle motions
299 could account for these. While this hypothesized contribution of the branchial arches remains
300 to be tested, our study demonstrates how sharks use coordinated cartilage motions to control
301 the motion of food through the oropharynx so that it can be successfully transported and
302 swallowed.

303

304 **Hyoid motion during transport**

305 Caudal food motion consistently corresponded with hyoid motion during the transport
306 behaviors observed in this study. Although the exact mechanism cannot be directly
307 determined from our data, our results are consistent with the food being moved by caudally-
308 directed water currents, generated by hyoid motion. In most trials, the food travelled caudally
309 towards the esophagus as the hyoid elevated with the mouth (gape) closed (Fig. 4). Hyoid
310 elevation compresses the oral cavity, and since the jaws are closed water—and food—will be
311 pushed caudally through the oropharynx and out of the opened fifth gill slit, which remains
312 open throughout most of the feeding events (Wilga and Sanford, 2008). Such compressive
313 transport behaviors occur in several elasmobranch species where the closed jaws, hyoid and
314 hypobranchial regions are elevated by nearly simultaneous activation of cranial muscles that
315 reduce the volume of the oropharyngeal cavity (Wilga and Motta, 1998a; Wilga and Motta,
316 1998b; Wilga et al., 2012). Thus, our results support the hypothesis that hyoid motion drives
317 food transport, via caudally-directed water flows within the oropharyngeal cavity (Dean et al.,
318 2005).

319 While all the sharks in this study used a step-wise food transport behavior, we did
320 observe some variation in the relationship between caudal food motion and hyoid motion. In
321 two of the seven trials, the food moved caudally as the hyoid depressed with the mouth open
322 in the first cycle of transport, and then switched to the pattern of caudal motion with hyoid

323 elevation and closed gape once the food had moved past the hyoid area (Fig. 4C, D). In one
324 trial (Fig. S2, Bam03 Trial02) the food remained in the hyoid region of the oropharyngeal
325 cavity for several seconds—moving caudally as the hyoid depressed and the mouth opened,
326 then rostrally with hyoid elevation for several cycles—before moving step-wise towards the
327 esophagus. This variation is likely due to the changing position of the food: while the food is
328 in the oral or hyoid region of the oropharynx (rostral to the hyoid), the food moves caudally
329 with hyoid depression (i.e., towards the hyoid). After moving into the pharynx (caudal to the
330 hyoid), food moves in a caudal direction (i.e., away from the hyoid) during hyoid elevation.
331 These patterns also suggest that sharks use a coordinated combination of hyoid and gape
332 motion to control the position and motion of food throughout the oropharynx.

333

334 **Pectoral girdle motion during transport**

335 We did not find evidence that motion of the pectoral girdle contributes substantially to food
336 transport in these sharks, as was hypothesized by Camp et al. (2017). First, pectoral girdle
337 depression and elevation motions during transport were relatively small—both compared to
338 the ceratohyal and to the pectoral girdle motions during the initial suction capture event—
339 suggesting its motion would contribute little to volume changes and therefore fluid flows in
340 the pharynx. Second, the relationship between pectoral girdle and food motion is not
341 consistent. During transport and swallowing, the coracoid bar elevated in or out of phase with
342 the motion of the hyoid and the food. This differed among individuals, and also within some
343 trials, and all individuals used both in and out of phase pectoral girdle rotation at least once.
344 While both in and out of phase hyoid and pectoral girdle compression could theoretically
345 drive anterior-to-posterior flows in the pharynx, it seems unlikely that a shark would switch
346 between these strategies during a single transport event. Coracoid bar depression did not
347 appear to hinder ceratohyal elevation even though these cartilages are connected by two
348 muscles in-series, the coracohyoideus and the coracoarcualis (Ramsay and Wilga, 2017).
349 While the pectoral girdle was mobile during food transport, the inconsistency of the phase
350 relationship between the hyoid and the pectoral girdle suggest that the pectoral girdle does
351 not drive caudal food motion, although it is possible that both of these motions could make
352 some contribution to food transport.

353

354 **Role of branchial arches in transport**

355 Although the caudal motion phases of food transport appear to be driven by hyoid elevation
356 (as described above), neither hyoid nor pectoral girdle motions can fully account for the
357 relatively immobile phases. In the pauses between caudal food motions, the hyoid
358 depresses. This should expand the oropharyngeal cavity and tend to pull water (and food)
359 back rostrally. However, the food is relatively stationary as the hyoid depresses, and we

360 observed minimal rostral translation of the food during this phase (Fig. 4). Pectoral girdle
361 motion is variable during these relatively immobile phases—either elevating or depressing—
362 and therefore unlikely to be stabilizing the food at this time. This suggests that the shark uses
363 some other structure or motion in these phases to prevent the food from being sucked back
364 rostrally.

365 Although we have no data on the branchial arches, it might be possible that these
366 cartilages adduct to hold the food between the basibranchial and hypobranchial cartilages in
367 the floor of the pharynx and the roof of the pharynx (Fig. 6). Vertical distance in the
368 pharyngeal cavity of white spotted bamboo sharks show that the pharyngobranchials and
369 basibranchials compress down to 2-4 mm apart during processing and transport events (C.J.
370 Wilga, unpublished data). While Fig. 6 show all the branchial arches compressed at the
371 same time, the gill slits and branchial arches can move independently (Dolce and Wilga,
372 2005; Karch et al., 2006; Wilga and Sanford, 2008) and could also compress in a wave-like
373 pattern. Hence, we hypothesize that the pharyngeal roof and floor compress to momentarily
374 stop the food. During this compression, the hyoid arch can depress again to start another
375 cycle of food transport without drawing the food rostrally, thus creating the step-wise motion
376 of the food toward the esophagus. In support of this theory, the epithelium lining the
377 oropharynx is studded with denticles (Atkinson et al., 2016) that could help increase friction
378 to grip the food. While we cannot directly test this hypothesis with the current dataset, the
379 lack of consistent hyoid or pectoral girdle motion to explain these relatively immobile phases
380 does support the branchial arches playing a role in food transport.

381

382 **Cartilage and food motion during swallowing**

383 It is clear that hyoid motion drives food transport through the oropharyngeal cavity, but
384 additional structures are likely contributing to swallowing. The velocity of the food during
385 swallowing is relatively high compared to the transport phase (Fig. 5). This high velocity
386 might suggest that food is carried to the esophagus by a water current (Fig. 5), although we
387 cannot test this hypothesis with our data as water flows were not measured. For example,
388 during the compressive transport of Atlantic guitarfish jaw elevation is proposed to generate
389 positive pressure and push food and water from the pharynx and presumably into the
390 esophagus (Wilga and Motta, 1998b). We did observe hyoid elevation just before swallowing,
391 but with a substantially smaller magnitude than during transport or capture (Fig. 4),
392 suggesting that hyoid motion alone is insufficient to explain the high velocity of food just
393 before swallowing. There was also little motion of the pectoral girdle during swallowing, so
394 we hypothesize that compression of the pharyngeal region could generate the water flow that
395 produces relatively high food velocities in the swallowing phase (Fig. 6), similar to that of
396 other elasmobranch species during compression transport (Wilga et al., 2012). However, as

397 the branchial arches were not visible in the X-ray videos and their motion could not be
398 measured, this hypothesis remains to be tested.

399

400 **Concluding Remarks**

401 Although based on a limited sample size, our results show how food is moved through the
402 oropharyngeal cavity and support previous studies by demonstrating that white-spotted
403 bamboo sharks can use coordinated motion of cartilages—from the jaws to the branchial
404 arches—to transport food. The step-wise motion of food via multiple cycles of hyoid elevation
405 may have been used by these sharks because of the relatively small size of the food items
406 (less than one half gape width). While larger food items may not elicit this step-wise food
407 transport, it could be used in other sharks that bite off small pieces of prey during feeding
408 and use compressive transport (Motta and Wilga, 2001; Wilga and Motta, 2000). Our results
409 lend further support to previous studies showing that hyoid-generated water currents drive
410 intraoral food transport in sharks, but also raise new hypotheses about the contribution of
411 branchial arch motion (especially dorsoventral compression) to food transport and
412 swallowing. Additional detailed studies of these structures are needed to determine their
413 specific role in allowing sharks to meet the challenge of transporting food through a relatively
414 long oropharyngeal cavity (compared to actinopterygians) without a muscular tongue or
415 pharyngeal jaws. Revealing the specific mechanisms of this step-wise motion of food during
416 transport and swallowing in Chondrichthyes will fill a major gap in our understanding the
417 functional diversity and evolution of these essential behaviors in gnathostome vertebrates
418 (Heiss et al., 2018).

419

420 **Acknowledgements**

421 We are grateful to Erika Tavares for her help in the X-ray filming, to Laura Vigil, Ben
422 Concepcion and Preston Steele for providing shark husbandry and training, David Baier for
423 the XROMM MayaTools, Kenneth Osborne for help with coding in R Studio, and two
424 anonymous reviewers for providing constructive comments. Lastly, we thank Nibs, Dipper
425 and Five Spot for their willingness to cooperate during the experiments.

426

427 **Competing interests**

428 The authors declare no competing or financial interests.

429

430 Funding

431 This work was supported by the US National Science Foundation [IOS-1655756 to E.L.B.
432 and A.L.C.; DBI-1661129 to E.L.B.; IOS-1354189 to C.A.D. and Graduate Research
433 Fellowships DGE-1644760 to E.B.K., A.R.M. and H.I.W.], Biotechnology and Biological
434 Sciences Research Council Future Leader Fellowship [A.L.C.], Brown University Presidential
435 Fellowships [A.R.M. and H.I.W.] University of Rhode Island Graduate Teaching
436 Assistantships [B.S.].

437

438 Data availability

439 Data for this publication have been deposited and opened for public use in the XMAPortal
440 (xmaportal.org), in the study ‘Bamboo Shark Feeding,’ with the permanent identifier URI1.
441 Video data are stored with their essential metadata in accordance with best practices for
442 video data management in organismal biology (Brainerd et al., 2017).

443

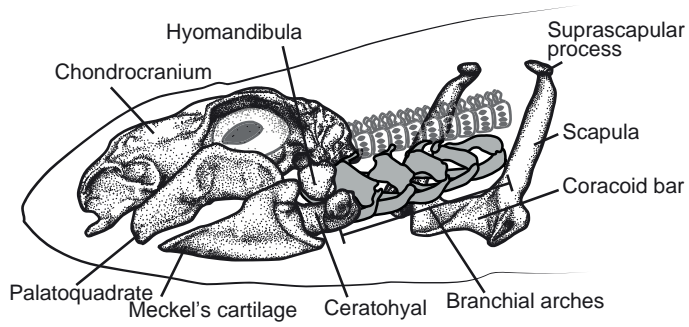
444 References

- 445 **Atkinson, C. J. L., Martin, K. J., Fraser, G. J. and Collin, S. P.** (2016). Morphology and
446 distribution of taste papillae and oral denticles in the developing oropharyngeal cavity of
447 the bamboo shark, *Chiloscyllium punctatum*. *Biol Open* **5**, 1759–1769.
- 448 **Bemis, W. E.** (1986). Feeding systems of living Dipnoi: anatomy and function. *J Morphol*
449 **190**, 249–275.
- 450 **Brainerd, E. L., Baier, D. B., Gatesy, S. M., Hedrick, T. L., Metzger, K. A., Gilbert, S. L.**
451 **and Crisco, J. J.** (2010). X-ray reconstruction of moving morphology (XROMM):
452 precision, accuracy and applications in comparative biomechanics research. *J Exp Zool*
453 *Part A* **313**, 262–279.
- 454 **Brainerd, E. L., Blob, R. W., Hedrick, T. L., Creamer, A. T. and Müller, U. K.** (2017). Data
455 management rubric for video data in organismal biology. *Integr Comp Biol* **57**, 33–47.
- 456 **Camp, A. L. and Brainerd, E. L.** (2014). Role of axial muscles in powering mouth expansion
457 during suction feeding in largemouth bass (*Micropterus salmoides*). *J Exp Biol* **217**,
458 1333.
- 459 **Camp, A. L., Scott, B., Brainerd, E. L. and Wilga, C. D.** (2017). Dual function of the
460 pectoral girdle for feeding and locomotion in white-spotted bamboo sharks. *P R Soc B*
461 **284**, 20170847.
- 462 **Dean, M. N., Wilga, C. D. and Summers, A. P.** (2005). Eating without hands or tongue:
463 specialization, elaboration and the evolution of prey processing mechanisms in
464 cartilaginous fishes. *Biol Lett.* **1**, 357–361.
- 465 **Dolce, J. L. and Wilga, C. D.** (2005). Gill slit kinematics in suction and ram ventilating
466 sharks. In *Integr Comp Biol*, p. 988.
- 467 **Gatesy, S. M., Baier, D. B., Jenkins, F. A. and Dial, K. P.** (2010). Scientific rotoscoping: a
468 morphology-based method of 3-D motion analysis and visualization. *J Exp Zool Part A*
469 **313**, 244–261.

- 470 **Gillis, G. and Lauder, G.** (1994). Aquatic prey transport and the comparative kinematics of
471 *Ambystoma tigrinum* feeding behaviors. *J Exp Biol* **187**, 159–179.
- 472 **Gillis, G. and Lauder, G.** (1995). Kinematics of feeding in bluegill sunfish: is there a general
473 distinction between aquatic capture and transport behaviors? *J Exp Biol* **198**, 709.
- 474 **Gussekkloo, S. W. S. and Bout, R. G.** (2005). The kinematics of feeding and drinking in
475 palaeognathous birds in relation to cranial morphology. *J Exp Biol* **208**, 3395–3407.
- 476 **Heiss, E., Aerts, P. and Van Wassenbergh, S.** (2018). Aquatic–terrestrial transitions of
477 feeding systems in vertebrates: a mechanical perspective. *J Exp Biol* **221**, jeb154427.
- 478 **Herrel, A., Cleuren, J. and Vree, F.** (1996). Kinematics of feeding in the lizard *Agama*
479 *stellio*. *J Exp Biol* **199**, 1727–1742.
- 480 **Herrel, A., Wauters, I., Aerts, P. and de Vree, F.** (1997). The mechanics of ovophagy in the
481 beaded lizard (*Heloderma horridum*). *J Herpetol* **31**, 383–393.
- 482 **Hiimae, K. M. and Crompton, A. W.** (1985). Mastication, food transport and swallowing. pp.
483 262–290.
- 484 **Kambic, R. E., Roberts, T. J. and Gatesy, S. M.** (2014). Long-axis rotation: a missing
485 degree of freedom in avian bipedal locomotion. *J Exp Biol* **217**, 2770.
- 486 **Karch, A. P., Dolce, J. L. and Wilga, C. D.** (2006). Gill slit kinematics during ventilation and
487 feeding in bamboo sharks. In *Integr Comp Biol*, p. E214.
- 488 **Kley, N. J. and Brainerd, E. L.** (2002). Post-cranial prey transport mechanisms in the black
489 pinesnake, *Pituophis melanoleucus lodingi*: an x-ray videographic study. *Zoology* **105**,
490 153–164.
- 491 **Knörlein, B. J., Baier, D. B., Gatesy, S. M., Laurence-Chasen, J. D. and Brainerd, E. L.**
492 (2016). Validation of XMA Lab software for marker-based XROMM. *J Exp Biol* **219**,
493 3701.
- 494 **Lauder, G. V.** (1983). Food capture. In *Fish biomechanics* (ed. Webb, P. W.) and Weihs, D.),
495 pp. 280–311. New York: Praeger.
- 496 **Levine, R. P., Monroy, J. A. and Brainerd, E. L.** (2004). Contribution of eye retraction to
497 swallowing performance in the northern leopard frog, *Rana pipiens*. *J Exp Biol* **207**,
498 1361–1368.
- 499 **Liem, K. F.** (1990). Aquatic versus terrestrial feeding modes: possible impacts on the trophic
500 ecology of vertebrates. *Am Zool* **30**, 209–221.
- 501 **Mehta, R. S. and Wainwright, P. C.** (2007). Raptorial jaws in the throat help moray eels
502 swallow large prey. *Nature* **449**, 79.
- 503 **Michel, K. B., Heiss, E., Aerts, P. and Van Wassenbergh, S.** (2015). A fish that uses its
504 hydrodynamic tongue to feed on land. *P R Soc B* **282**, 20150057.
- 505 **Motta, P. J. and Wilga, C. D.** (2001). Advances in the study of feeding behaviors,
506 mechanisms, and mechanics of sharks. *Env. Biol Fish* **60**, 131–156.
- 507 **Natchev, N., Heiss, E., Lemell, P., Stratev, D. and Weisgram, J.** (2009). Analysis of prey
508 capture and food transport kinematics in two Asian box turtles, *Cuora amboinensis* and
509 *Cuora flavomarginata* (Chelonia, Geoemydidae), with emphasis on terrestrial feeding
510 patterns. *Zoology* **112**, 113–127.
- 511 **Nauwelaerts, S., Wilga, C. D., Sanford, C. P. and Lauder, G. V.** (2007). Hydrodynamics of
512 prey capture in sharks: effects of substrate. *J R Soc Interface* **4**, 341–345.

- 513 **Nauwelaerts, S., Wilga, C. D., Lauder, G. V and Sanford, C. P.** (2008). Fluid dynamics of
514 feeding behaviour in white-spotted bamboo sharks. *J Exp Biol* **211**, 3095–3102.
- 515 **Ramsay, J. B. and Wilga, C. D.** (2017). Function of the hypobranchial muscles and
516 hyoidmandibular ligament during suction capture and bite processing in white-spotted
517 bamboo sharks, *Chiloscyllium plagiosum*. *J Exp Biol* jeb. 165290.
- 518 **Reilly, S. M. and Lauder, G. V** (1990). The evolution of tetrapod feeding behavior: kinematic
519 homologies in prey transport. *Evolution (N. Y.)*. **44**, 1542–1557.
- 520 **Schaerlaeken, V., Montuelle, S. J., Aerts, P. and Herrel, A.** (2011). Jaw and hyolingual
521 movements during prey transport in varanid lizards: effects of prey type. *Zoology* **114**,
522 165–170.
- 523 **Scott, B., Wilga, C. A. D. and Brainerd, E. L.** (2019). Skeletal kinematics of the hyoid arch
524 in a suction-feeding shark, *Chiloscyllium plagiosum*.
- 525 **Vandewalle, P., Parmentier, E. and Chardon, M.** (2000). The branchial basket in Teleost
526 feeding. *Cybium* **24**, 319–342.
- 527 **Wainwright, P. C.** (2005). Functional morphology of the pharyngeal jaw apparatus. *Fish*
528 *Physiol* **23**, 77–101.
- 529 **Werth, A.** (2000). Feeding in Marine Mammals. In *Feeding: form, function and evolution in*
530 *tetrapod vertebrates*, pp. 487–526.
- 531 **Wilga, C. D.** (2008). Evolutionary divergence in the feeding mechanism of fishes. *Acta Geol*
532 *Pol* **58**, 113–120.
- 533 **Wilga, C. D.** (2010). Hyoid and pharyngeal arch function during ventilation and feeding in
534 elasmobranchs: conservation and modification in function. *J Appl Ichthyol* **26**, 162–166.
- 535 **Wilga, C. D. and Motta, P. J.** (1998a). Conservation and variation in the feeding mechanism
536 of the spiny dogfish *Squalus acanthias*. *J Exp Biol* **201**, 1345–1358.
- 537 **Wilga, C. D. and Motta, P. J.** (1998b). Feeding mechanism of the Atlantic guitarfish
538 *Rhinobatos lentiginosus*: modulation of kinematic and motor activity. *J Exp Biol* **201**,
539 3167–3183.
- 540 **Wilga, C. D. and Motta, P. J.** (2000). Durophagy in sharks: feeding mechanics of the
541 hammerhead *Sphyrna tiburo*. *J Exp Biol* **203**, 2781–2796.
- 542 **Wilga, C. D. and Sanford, C. P.** (2008). Suction generation in white-spotted bamboo sharks
543 *Chiloscyllium plagiosum*. *J Exp Biol* **211**, 3128–3138.
- 544 **Wilga, C. D., Motta, P. J. and Sanford, C. P.** (2007). Evolution and ecology of feeding in
545 elasmobranchs. *Integr Comp Biol* **47**, 55–69.
- 546 **Wilga, C. D., Stoehr, A. A., Duquette, D. C. and Allen, R. M.** (2012). Functional ecology of
547 feeding in elasmobranchs. *Env. Biol Fish* **95**, 155–167.
- 548 **Zweers, G. A., Berkhoudt, H. and Vanden Berge, J. C.** (1994). Behavioral mechanisms of
549 avian feeding. In *Biomechanics of feeding in vertebrates*, pp. 241–279. Springer.
- 550

551 Figure legends

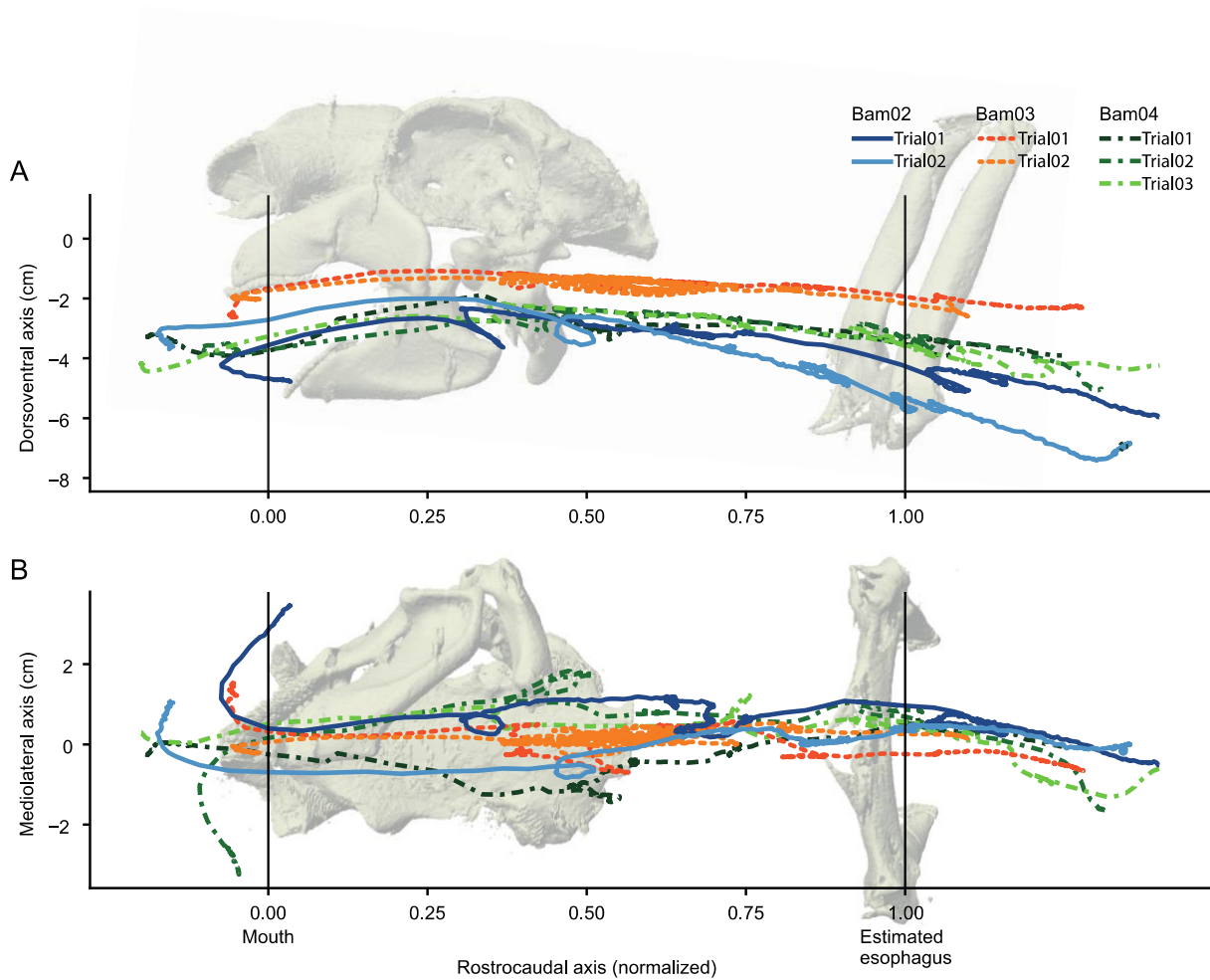


552

553 **Figure 1: The feeding apparatus of a white-spotted bamboo shark, *Chiloscyllium plagiosum*.** The coracoid
554 bar, scapulae, and suprascapular processes together form the scapulocoracoid or pectoral girdle. The muscles
555 and most of the right-side cartilages have been left out for clarity. The grey branchial arches are in a natural,
556 dorsoventrally compressed posture in this image, based on CT scans. Figure modified from (Camp et al., 2017).
557

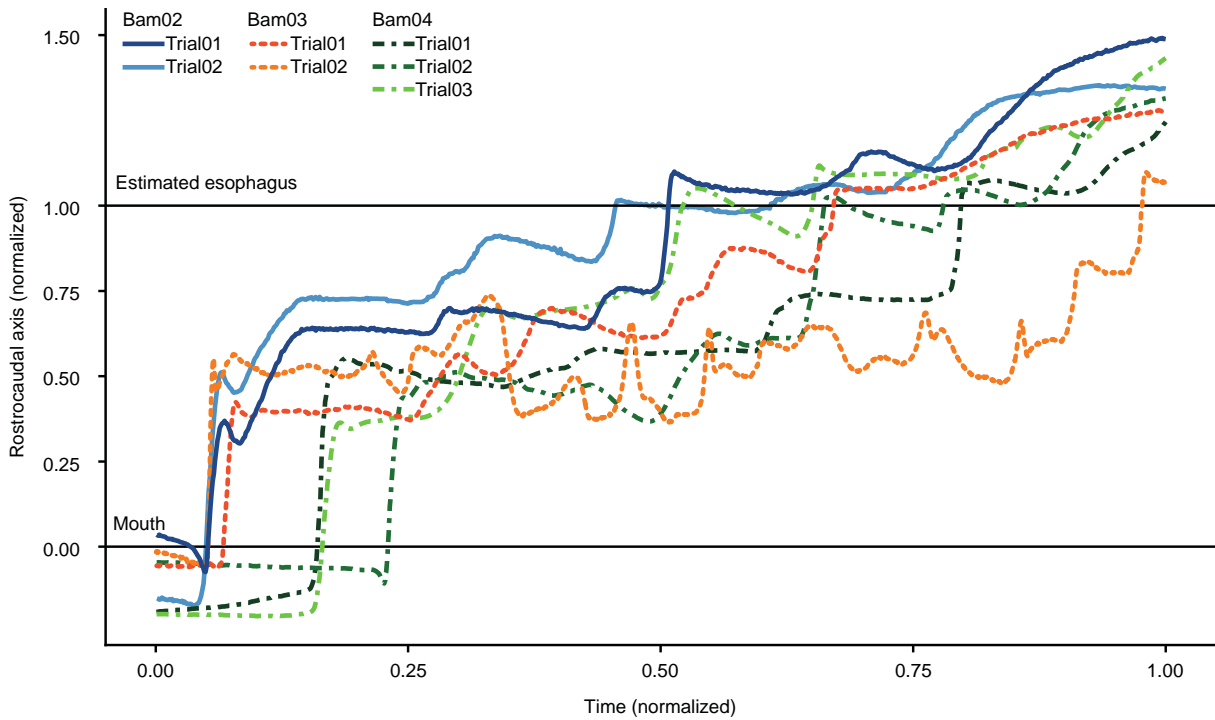
558

559



560

561 **Figure 2: Food trajectories measured relative to the chondrocranium from a (A) lateral view and (B)**
562 **ventral view.** The colors correspond to individual trials (see legend), with trials from Bam02 in blues, Bam03 in
563 reds, and Bam04 in greens (total n = 7). The x-axis represents the food's position along the rostrocaudal axis
564 where x = 0.0 and x = 1.0 represent the mouth and pectoral girdle/esophagus, respectively. Images of the marked
565 cartilages (including only the left-side mandibular and hyoid arches) of Bam04 at peak gape are included as an
566 approximate guide to the food's position. Because sharks have flexibility in the relative positions of their
567 chondrocranium and pectoral girdle from trial to trial, it appears in A as if the opening to the esophagus is very
568 large, but this is not the case. The dorsoventral range of food location as it passes the pectoral girdle is an artifact
569 of plotting these trajectories relative to the chondrocranium; plotting food motion relative to the pectoral girdle
570 would show the opening to the esophagus more clearly but produce artifacts at the mouth.



571

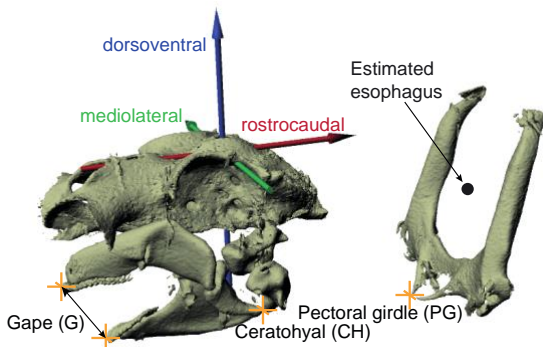
572 **Figure 3: Rostrocaudal translation of the food relative to the cranium as a function of normalized time.**

573 The y-axis represents the food's position along the rostrocaudal axis where $y=0.0$ and $y=1.0$ represent the mouth

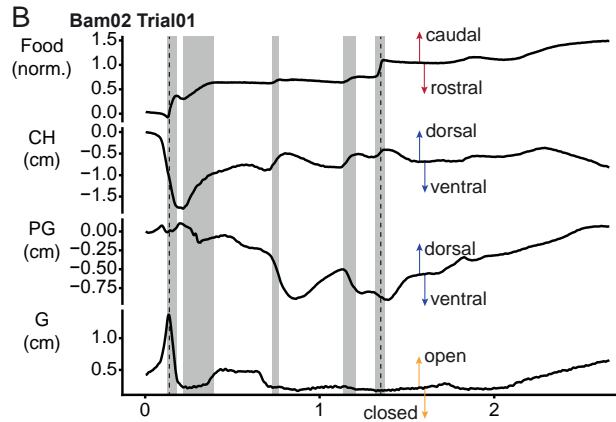
574 and pectoral girdle, respectively, as in the x-axis of Fig. 2. Time was normalized to trial length for comparison

575 among trials. Line colors correspond to trials and individuals, following Fig 2.

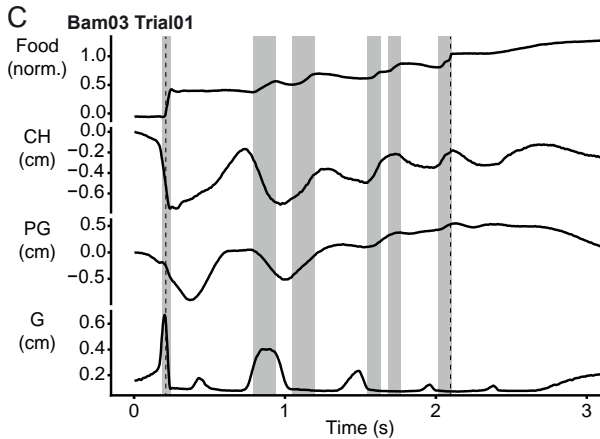
A



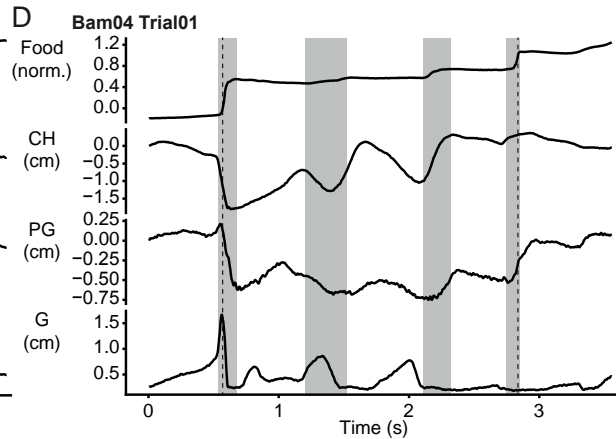
B



C



D

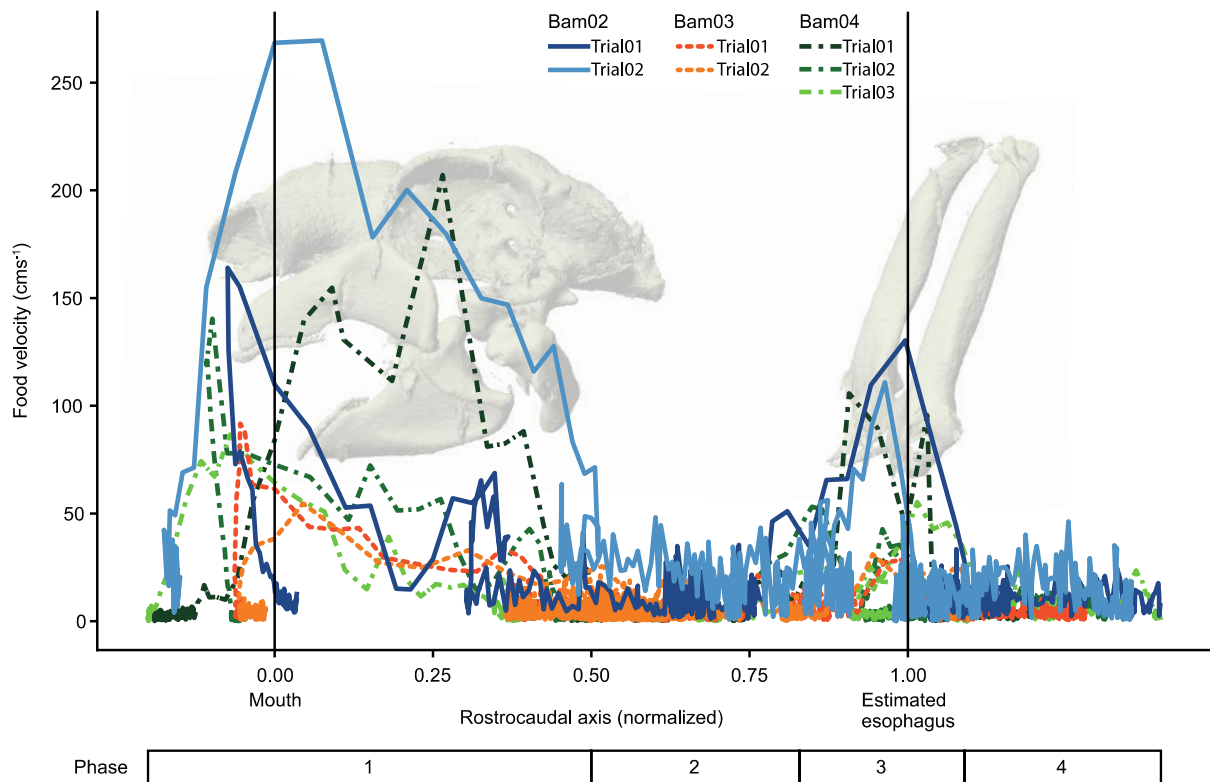


576

577 **Figure 4: Rostrocaudal translations of food, displacements of ceratohyal and pectoral girdle, and gape**

578 **width over time in a sample trial from each individual. A) Cartilages of Bam04 at peak gape, showing the**

579 virtual landmarks (yellow), the chondrocranium ACS (green, blue, and red arrows), and estimated esophagus
 580 location (black circle). B-D) Plots of food and cartilage movements and gape. With the exception of gape, all
 581 movements were calculated relative to the chondrocranium ACS. The shaded bars represent periods of caudally-
 582 directed food translation, and the vertical dotted lines represent the times when the food passes the jaw tips and
 583 the pectoral girdle (on the food y-axis, where $y = 0.0$ and $y = 1.0$, respectively). The directional arrow colors in B
 584 correspond to the arrow colors of the ACS in A. All trials are shown in Fig. S2. Abbreviations: Food (norm),
 585 normalized translation of food on the rostrocaudal axis; CH, displacement of the rostroventral tip of the ceratohyal
 586 in the dorsoventral direction (cm); PG, displacement of the ventral tip of the pectoral girdle (cm) in the
 587 dorsoventral direction; G, gape width, calculated from the distance between the jaw tips (cm).

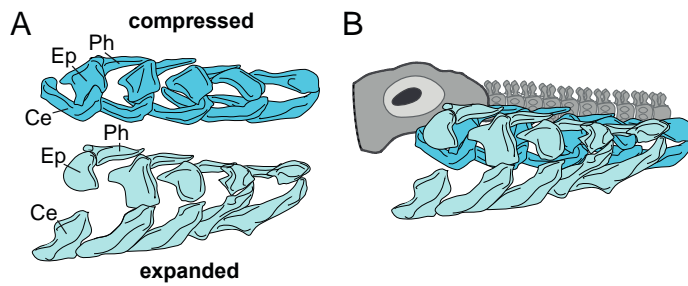


588 Phase

1	2	3	4
---	---	---	---

589 **Figure 5: Rostrocaudal velocity of the food relative to its position within the oropharynx.** The marked
 590 cartilages in the background serve as an indicator of the approximate position of the food within the animal. As in
 591 Fig. 2, the x-axis represents the food's position along the rostrocaudal axis where $x=0.0$ and $x=1.0$ represent the
 592 mouth and pectoral girdle, respectively. Line colors correspond to trials and individuals, following Fig. 2. Food
 593 motion occurred in four phases: Phase 1: prey capture, phase 2: oropharyngeal transport, phase 3: swallowing,
 594 phase 4: after swallowing.
 595

596



597

598 **Figure 6: Lateral-view diagram of the branchial arch anatomy and positions.** (A) Left-side of the branchial
599 arches in the compressed (dark blue, top) and expanded (light blue) positions from CT scans. Shown in lateral
600 view with rostral to the left. Ph: Pharyngobranchials, Ep: Epibranchials, Ce: Ceratobranchials. The ventralmost
601 elements of the arches that make up the floor of the pharynx, the basibranchials and hypobranchials, are not
602 visible. (B) Lateral view of the branchial arches (in blues), relative to the cranium and vertebral column (in grey).
603